DOI: 10.1002/ejic.200501092

New Heterometallic (Cu^{II} and Cr^{III}) Complexes – First Crystal Structure of an Oxalate-Bridged Ferromagnetically Coupled [$Cu^{II}Cr^{III}Cu^{II}$] System

Marijana Jurić,[a] Pavica Planinić,[a] Nevenka Brničević,*[a] Dalibor Milić,[b] Dubravka Matković-Čalogović,[b] Damir Pajić,[c] and Krešo Zadro[c]

Keywords: Crystal structure / Copper complexes / Chromium complexes / Oxalate bridges / Ferromagnetic interaction

Two new heterotemetallic complexes [{Cu(μ-C_2O_4)(bpy)$_2$}$_2$-Cr(C_2O_4)]NO_3·H_2O (**1**) and [Cu(bpy)$_3$][Cr(C_2O_4)$_3$]NO_3·$9H_2O$ (**2**) (bpy = 2,2′-bipyridine) have been synthesized. The crystal structures were determined and magnetic and spectroscopic (IR, UV/Vis) characterization accomplished. In **1**, the central [Cr(C_2O_4)$_3$]$^{3-}$ unit acts as a bridge between two copper(II) ions, each of them having a distorted octahedral geometry. The apical positions are occupied by one oxygen atom belonging to the bridging oxalate anion [Cu–O2 = 2.6439(18) Å] and one nitrogen atom from one of the bpy ligands [Cu–N1 = 2.1079(18) Å]. The N_3O equatorial environment consists of three bpy nitrogen atoms [Cu–N = 1.995 Å (mean value)] and the second oxygen atom from the bridging oxalate anion [Cu–O1 = 2.1168(15) Å]. The chromium(III) atom is in a slightly distorted octahedral environment of four oxygen atoms from two bridging oxalate groups [Cr–O = 1.988 Å (mean value)] and two oxygen atoms from the terminally bonded bidentate oxalate group [Cr–O = 1.9454(16) Å]. Complex **2** consists of two mononuclear [Cu(bpy)$_3$]$^{2+}$ cations, one mononuclear [Cr(C_2O_4)$_3$]$^{3-}$ anion, one NO_3^- anion and nine molecules of water of crystallisation. The copper(II) ions in two crystallographically independent [Cu(bpy)$_3$]$^{2+}$ cations are in a tetragonally distorted octahedral coordination environment of six N atoms from the bpy ligands. The chromium(III) ion in [Cr(C_2O_4)$_3$]$^{3-}$ has a slightly distorted octahedral environment of oxygen atoms from three oxalate groups [with the Cr–O bond lengths ranging from 1.964(3) to 1.982(3) Å]. Analysis of the magnetic properties (1.8–290 K) of **1** showed a ferromagnetic exchange interaction between Cu^{II} and Cr^{III} with J = +1.20 cm^{-1} [using $\mathbf{H}_{INT} = -J(S_{Cu1}S_{Cr} + S_{Cu2}S_{Cr})$].

Introduction

The design of molecule-based magnetic materials has become one of the most stimulating challenges for chemists nowadays.[1,2] A generally accepted strategy for synthesizing these materials consists of assembling paramagnetic metal centres in such a way that the resulting solid lattices, with their components properly arranged, exhibit desired physical properties such as magnetic exchange interactions. In designing homo- and heteropolynuclear complexes, a very essential role belongs to the oxalate ion, $C_2O_4^{2-}$, because of its ability to adopt a bis(chelating) coordination mode as well as to mediate magnetic interactions between paramagnetic metal centres. On this account, stable mononuclear anionic oxalate complexes are often used as ligands toward the second metal ion, an approach known as "complexes as ligands" or "building-blocks chemistry".

One of the possibilities for the synthesis of molecule-based ferromagnetic materials, developed in the early 1990's, is based on the use of the tris(oxalato)chromate(III) anion, [Cr(C_2O_4)$_3$]$^{3-}$,[3] as one of the starting components. The advantage of using this anion is its stability towards ligand substitution as well as good control over the reaction products. By using [Cr(C_2O_4)$_3$]$^{3-}$ as a building block, a series of mixed-metal assemblies {[NR_4][$M^{II}Cr^{III}$(C_2O_4)$_3$]}$_n$ (R = *n*-butyl; M^{II} = Mn, Fe, Co, Ni, Cu, Zn) was obtained, for which the ferromagnetic phase transition was observed up to 14 K;[3a] the crystal structures of these assemblies were not known. Shortly afterwards, determination of the crystal structures of {[NR_4][$Mn^{II}Cr^{III}$(C_2O_4)$_3$]}$_n$ (R = *n*-butyl, *n*-propyl)[4] and {[PR_4][$Mn^{II}Cr^{III}$(C_2O_4)$_3$]}$_n$ (R = phenyl)[5] revealed a 2D structure, and ferromagnetic behaviour was confirmed. The anion [Cr(C_2O_4)$_3$]$^{3-}$ was also used in the preparation of the cubic 3D coordination polymers [$M^{I}Cr^{III}$(C_2O_4)$_3$]$_n^{2n-}$ (M^{I} = Li, Na)[6] or [$M^{II}Cr^{III}$-(C_2O_4)$_3$]$_n^{n-}$ (M^{II} = Mn, Fe, Co, Ni, Cu, Zn)[7] in which the charge was counterbalanced by a tris(chelated) transition-metal (M′) diimine, [M′(bpy)$_3$]$^{m+}$ (bpy = 2,2′-bipyridine; *m* = 2, 3). Other anionic oxalate complexes of chromium(III)

[a] Ruđer Bošković Institute,
Bijenička cesta 54, 10000, Zagreb, Croatia
[b] Department of Chemistry, Faculty of Science, University of Zagreb,
Horvatovac 102a, 10000, Zagreb, Croatia
[c] Department of Physics, Faculty of Science, University of Zagreb,
Bijenička cesta 32, 10000, Zagreb, Croatia

Supporting information for this article is available on the WWW under http://www.eurjic.org or from the author.

have also served as building blocks: the mono(oxalato) complexes $[CrL(C_2O_4)]^-$ [L = *N*,*N*′-ethylenebis(salicylideneaminate)][8] and $[CrL_2(C_2O_4)]^-$ (L = acetylacetonate)[9] have been used for the synthesis of heterodinuclear compounds, whereas the bis(oxalato) complexes $[CrL(C_2O_4)_2]^-$ (L = 2,2′-bipyridine,[10] 1,10-phenanthroline,[10d,11] 2,2′-bipyrimidine[12]) produced heterodinuclear as well as heteropolynuclear species of different dimensionalities.

Recently, the $[Cr(C_2O_4)_3]^{3-}$ and $[Fe(C_2O_4)_3]^{3-}$ anions were used in the synthesis of some oxalate-bridged trinuclear complexes such as $[Cu_2M^{III}(C_2O_4)_3(Mephen)_2]ClO_4$ (M^{III} = Cr, Fe; Mephen = 5-methyl-1,10-phenanthroline).[13a] The magnetic susceptibility data revealed an intramolecular ferromagnetic interaction between the copper(II) and chromium(III) ions through the oxalate bridge and an antiferromagnetic interaction between the copper(II) and iron(III) centres with spin-coupling constants of $+14.9\ cm^{-1}$ and $-12.7\ cm^{-1}$ [using $\mathbf{H}_{INT} = -2J(S_{Cu1}S_M + S_{Cu2}S_M)$], respectively. Slightly reduced values were obtained for similar complexes when Mephen was substituted by tmen (*N*,*N*,*N*′,*N*′-tetramethylethylenediamine).[13b] The occurrence of intramolecular ferromagnetic interactions between the copper(II) and chromium(III) ions through the oxalate bridge with spin-coupling constants of $+6.36\ cm^{-1}$ and $+7.02\ cm^{-1}$ [using $\mathbf{H}_{INT} = -2J(S_{Cu1}S_{Cr} + S_{Cu2}S_{Cr} + S_{Cu3}S_{Cr})$], has also been found for the tetranuclear complexes $[Cu_3Cr(C_2O_4)_3L_3](ClO_4)_3$ with L = diaminoethane and 1,3-diaminopropane, respectively.[13c] All of these complexes[13] were prepared as polycrystalline solids. Because of the lack of single crystals suitable for X-ray structural analysis, their structures remain unknown.

In relation to our current magneto-structural studies on the polynuclear transition-metal complexes, we report in this paper on two new heterometallic complexes, $[\{Cu(\mu\text{-}C_2O_4)(bpy)_2\}_2Cr(C_2O_4)]NO_3\cdot H_2O$ (**1**) and $[Cu(bpy)_3]_2[Cr(C_2O_4)_3]NO_3\cdot 9H_2O$ (**2**), which have been obtained by using the $[Cr(C_2O_4)_3]^{3-}$ anion as building block. To the best of our knowledge, the complex $[\{Cu(\mu\text{-}C_2O_4)(bpy)_2\}_2Cr(C_2O_4)]NO_3\cdot H_2O$ is, so far, the first heterotrinuclear oxalate-bridged copper(II)–chromium(III)–copper(II) compound for which the crystal structure has been determined. The structural data of the complexes have been correlated with magnetic and other measurements.

Results and Discussion

Preparation

Complex **1** was obtained in the form of dark-green crystals from the reaction of aqueous solutions of $K_3[Cr(C_2O_4)_3]\cdot 3H_2O$ and $Cu(NO_3)_2\cdot 3H_2O$ and an ethanolic solution of 2,2′-bipyridine in the ratio 1:2:4. Single crystals of **2** were formed as the only solid by slow concentration of the aqueous solution containing $K_3[Cr(C_2O_4)_3]\cdot 3H_2O$ and $[Cu(bpy)_3](NO_3)_2\cdot 6H_2O$ in the ratio 1:1. When this reaction was performed with a 1:2 ratio of the precursors, crystals of **1** and **2** formed simultaneously. Both compounds are moderately stable in air and rather insoluble in common organic solvents.

Description of the Structures

[{Cu(μ-C$_2$O$_4$)(bpy)$_2$}$_2$Cr(C$_2$O$_4$)]NO$_3$·H$_2$O (1)

The structure of **1** consists of trinuclear $[\{Cu(\mu\text{-}C_2O_4)(bpy)_2\}_2Cr(C_2O_4)]^+$ cations, nitrate anions and uncoordinated water molecules. The trinuclear cation (Figure 1) can be considered as being composed of two $[Cu(bpy)_2]^{2+}$ moieties bridged by the $[Cr(C_2O_4)_3]^{3-}$ complex anion, which acts as a bidentate ligand towards each of the copper atoms.

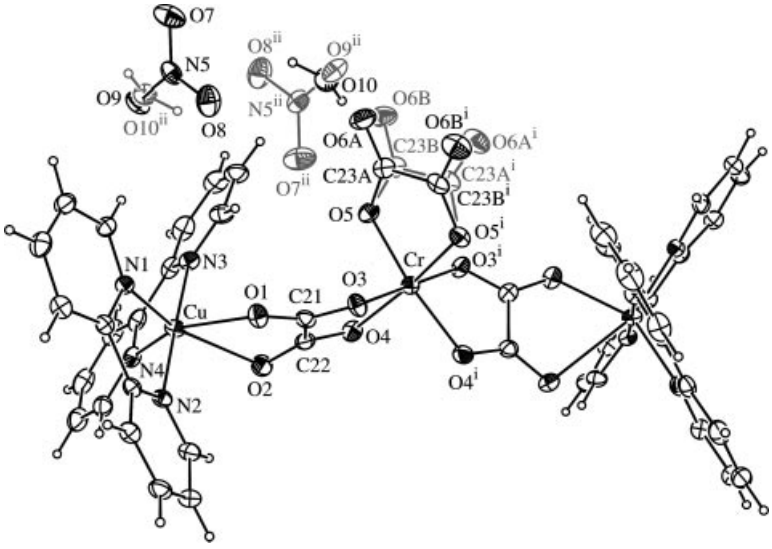

Figure 1. Asymmetric unit of **1** with atom numbering scheme and displacement ellipsoids drawn at the 50% probability level. Two halves of the $[\{Cu(\mu\text{-}C_2O_4)(bpy)_2\}_2Cr(C_2O_4)]^+$ cation are related by the symmetry operator (i) $1-x, y, 1/2-z$. The carboxylate groups of the terminal oxalate ligand are disordered (see text for explanation). The water molecule and nitrate ion are disordered over two sites related by the symmetry operator (ii) $1-x, -y, -z$. Atoms in the alternative sites and their numbering scheme are shown in grey.

Although compound **1** crystallises in the space group *C*2/*c* (see Exp. Sect.) with the chromium atom situated on the twofold axis, the trinuclear cation possesses only approximate C_2 symmetry: atoms C23 and O6 of the terminal oxalate group (which is intersected by the crystallographic twofold axis) are disordered over two sites (denoted A and B). The distance between C23A and the equivalent atom generated by the twofold symmetry C23A(1 – *x*, *y*, 1/2 – *z*) is 1.657(18) Å, whereas the distance C23A–C23B(1 – *x*, *y*, 1/2 – *z*) is 1.572(18) Å and is closer to the value for a C–C single bond.[14] This suggests that the two atoms from one of the carboxylate groups are in the A site and the corresponding atoms from the other carboxylate group of the terminal oxalate ligand are in the B site (Figure 1). This oxalate group is, therefore, statistically disordered, and the occupancies of the C23A, C23B, O6A and O6B atoms were fixed at 0.50 during refinement. Furthermore, the lattice water molecules and nitrate ions are disordered over two sites related by the inversion centre, so that the occupancy of each site equals exactly one half (Figure 1).

The apical positions in the distorted octahedron around Cu are occupied by the O2 and N1 atoms. The Cu–O2 bond [2.6439(18) Å] is significantly longer than the Cu–O1 bond [2.1168(15) Å]. The Cu–N1 bond [2.1079(18) Å] is the longest one among the four Cu–N bonds (Table 1). The remaining three bpy nitrogen (N2, N3 and N4) atoms having an average Cu–N bond length of 1.995 Å as well as the O1 atom are located in the equatorial plane. The pyridyl rings of the bpy ligands are slightly tilted towards each other. The dihedral angles between the planes of the pyridyl rings are 15.78(10)° (for the bpy ligand including N1 and N2) and 4.52(11)° (for the ligand including N3 and N4).

Table 1. Selected bond lengths [Å] and angles [°] for compound **1**.

Cu–O1	2.1168(15)	Cu–N1	2.1079(18)
Cu–O2	2.6439(18)	Cu–N2	1.9774(19)
Cr–O3	1.9866(16)	Cu–N3	1.9663(19)
Cr–O4	1.9900(16)	Cu–N4	2.0423(19)
Cr–O5	1.9454(16)		
O3–Cr–O4	82.52(7)	O1–Cu–N3	92.59(7)
O3–Cr–O5	90.79(7)	O1–Cu–N4	148.62(7)
O3–Cr–O3^{i}[a]	179.51(7)	O2–Cu–N1	162.09(6)
O3–Cr–O4^{i}	97.14(7)	O2–Cu–N2	101.23(7)
O3–Cr–O5^{i}	89.57(7)	O2–Cu–N3	78.23(7)
O4–Cr–O5	93.17(7)	O2–Cu–N4	78.32(6)
O4–Cr–O4^{i}	91.14(7)	N1–Cu–N2	80.68(7)
O4–Cr–O5^{i}	171.41(7)	N1–Cu–N3	99.37(7)
O5–Cr–O5^{i}	83.56(7)	N1–Cu–N4	119.13(7)
O1–Cu–O2	70.30(6)	N2–Cu–N3	178.42(7)
O1–Cu–N1	92.22(6)	N2–Cu–N4	99.87(8)
O1–Cu–N2	85.83(7)	N3–Cu–N4	81.49(8)

[a] Symmetry code: (i) 1 – *x*, *y*, 1/2 – *z*.

The Cr atom in **1** is bonded to six oxygen atoms arranged in a slightly distorted octahedron. As already observed in similar complexes,[10a,15,16] the Cr–O bonds are longer for the bridging oxalate ligands [1.9866(16) Å and 1.9900(16) Å] than for the terminal one [1.9454(16) Å], but they are all shorter than the Cu–O bonds (Table 1). The carboxylate groups of the oxalate ligands are not coplanar; instead, they are rotated around the C–C bond by 14.05(12)° in the bridging ligands and by 6.0(17)° in the terminal one.

The complex cations, mutually related by the twofold axis, are stacked in columns parallel to the *c* axis because of the offset π–π interactions between pyridyl moieties. The columns of the complex cations are further connected with the neighbouring columns by zipper-like offset π–π stacking interactions between the pyridyl moieties: in this way, layers parallel to (010) are formed. These layers consist of pyridyl rings with two different orientations alternating in the *a*-direction: (a) the rings almost parallel to (012) and (b) those almost parallel to (01$\bar{2}$) (Figure 2). The contact distances between atoms involved in the pyridyl π–π stacking interactions range from 3.324(3) Å to 3.594(3) Å, which indicates that these are strong to modest π–π interactions.[17] The two layers of the complex cations are held together by the C–H···O hydrogen bonds and other interactions mediated by the nitrate ions and water molecules: each water molecule bridges the complex cation and the nitrate anion by forming two hydrogen bonds: O10–H101···O6A of 2.92(2) Å and O10–H102···O8 of 2.814(19) Å, (Figure 3; Table 2). Additionally, the carboxylate group of the terminal oxalate ligand occupying the B site and the nitrate ion are in close contact [N5···O6B(1 – *x*, –*y*, –*z*) = 3.201(7) Å; O7···C23B(1 – *x*, –*y*, –*z*) = 3.103(14) Å] and exhibit a π–π stacking interaction [the angle between the plane of the nitrate ion and that of the carboxylate group B equals 18.7(9)°]. In the proposed structural model, the carboxylate group nearest to the nitrate ion always occupies the B site; otherwise, unacceptably short contacts between the nitrate ion and carboxylate group at the A site [N5···O6A(1 – *x*, –*y*, –*z*) = 2.588(8) Å; O7···C23A(1 – *x*, –*y*, –*z*) = 2.775(16) Å] would be present.

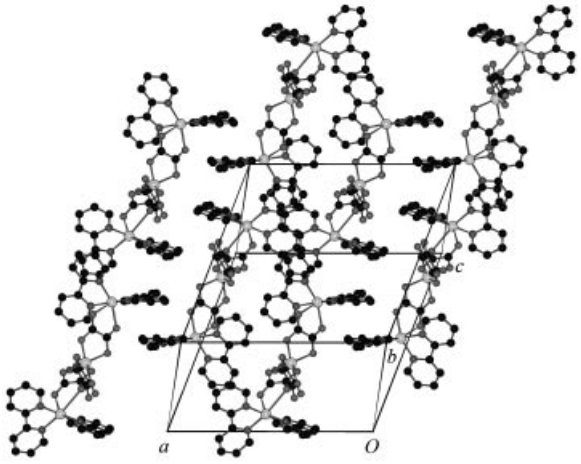

Figure 2. Pyridyl π–π stacking in **1**. The stacking almost parallel to (012) alternates in the *a*-direction with the stacking almost parallel to (01$\bar{2}$). Hydrogen atoms are omitted for clarity.

The Cu···Cr distance across the bridging oxalate group is 5.4605(5) Å. It is similar to the corresponding values found elsewhere: in the dinuclear complex [(bpy)(C_2O_4)Cr-(μ-C_2O_4)Cu(Hfsaaep)(H_2O)]·2H_2O {H_2fsaaep = 3-[*N*-2-(pyridylethyl)formimidoyl]salicylic acid; Cu···Cr =

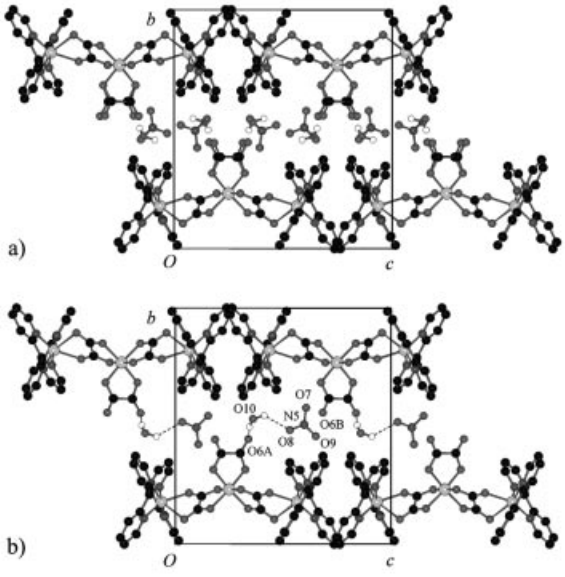

Figure 3. The cavities between two layers of the trinuclear cations in **1** are filled with nitrate ions and water molecules. Hydrogen atoms attached to the carbon atoms are omitted for clarity. (a) Each water–nitrate pair is disordered over two sites related by the inversion centre. (b) One of two possible orientations of the water–nitrate pairs in the cavities in a row, mutually related by the glide plane *c*.

Table 2. O–H···O hydrogen-bonding interactions in compound **1**.

D–H···A	D–H [Å]	H···A [Å]	D···A [Å]	D–H···A [°]
O10–H101···O6A	0.80	2.20	2.92(2)	150
O10–H102···O8	0.88	2.15	2.814(19)	132

5.506 Å},[16] in the trinuclear complex $[CuCr_2(bpy)_2(C_2O_4)_4(H_2O)_2]\cdot 1.5H_2O$ (Cu···Cr = 5.288 Å)[10a] or in the tetranuclear compound $[Cr_2Cu_2(bpy)_4(C_2O_4)_5]\cdot 2H_2O$ [Cu···Cr = 5.4473(17) Å].[15b] The oxalate bridging mode in all of these complexes is the same as that in **1**. The shortest intermolecular Cu···Cu, Cu···Cr and Cr···Cr distances in the structure of **1** are 6.0311(6) Å [Cu···Cu(1 – *x*, *y*, –1/2 – *z*)], 7.6473(8) Å [Cu···Cr(1 – *x*, 1 – *y*, –*z*)] and 9.4527(7) Å [Cr···Cr(3/2 – *x*, 1/2 – *y*, 1 – *z*)], respectively.

[Cu(bpy)$_3$]$_2$[Cr(C$_2$O$_4$)$_3$]NO$_3$·9H$_2$O (2)

The asymmetric unit of **2** is composed of two mononuclear, crystallographically independent $[Cu(bpy)_3]^{2+}$ cations, a mononuclear $[Cr(C_2O_4)_3]^{3-}$ anion, a nitrate anion and nine molecules of water of crystallisation, two of which are disordered over two positions (Figure 4). Each copper atom is coordinated by six nitrogen atoms of the three chelating bpy ligands. The two axial Cu–N bonds in each of the $[Cu(bpy)_3]^{2+}$ cations [Cu1–N2 = 2.247(3) Å and Cu1–N5 = 2.291(3) Å; Cu2–N8 = 2.171(3) Å and Cu2–N11 = 2.200(4) Å] are significantly longer than the other four [ranging from 2.027(3) Å to 2.055(5) Å for Cu1 and from 2.068(5) Å to 2.088(5) Å for Cu2; Table 3]; thus an elongated octahedron is formed (as expected as a result of the Jahn–Teller effect). The dihedral angles between pyridyl moieties are smaller for the ligands coordinated to Cu1 [5.0(3)°, 5.19(18)° and 6.23(19)°] than for those coordinated to Cu2 [10.4(2)°, 9.76(19)° and 6.6(3)°]. The geometrical parameters of $[Cu(bpy)_3]^{2+}$ in **2** are significantly different from those found in some other $[Cu(bpy)_3]^{2+}$ complexes {the apical Cu–N distances in $[Cu(bpy)_3][Ni(tdtdt)_2]_2$ (tdtdt = 2-thioxo-1,3-dithiole-4,5-dithiolate)[18] are longer than the equatorial ones by only 0.02 Å; the octahedral geometry in $[Cu(bpy)_3](ClO_4)_2$[19] is more distorted than in **2**; the coordination polyhedron around Cu in $[Cu(bpy)_3][Hg_2I_6]$[20] is a flattened octahedron}, but they are similar to those found in $[Cu(dmbpy)_3](BF_4)_2\cdot C_2H_5OH$, where the ligand dmbpy indicates 5,5-dimethyl-2,2′-bipyridine.[21] The Cr atom in $[Cr(C_2O_4)_3]^{3-}$ is coordinated by six oxygen atoms of the three bidentate oxalate ligands in a slightly distorted octahedral arrangement. The Cr–O bond lengths range from 1.964(3) Å to 1.982(3) Å, and the structure of the

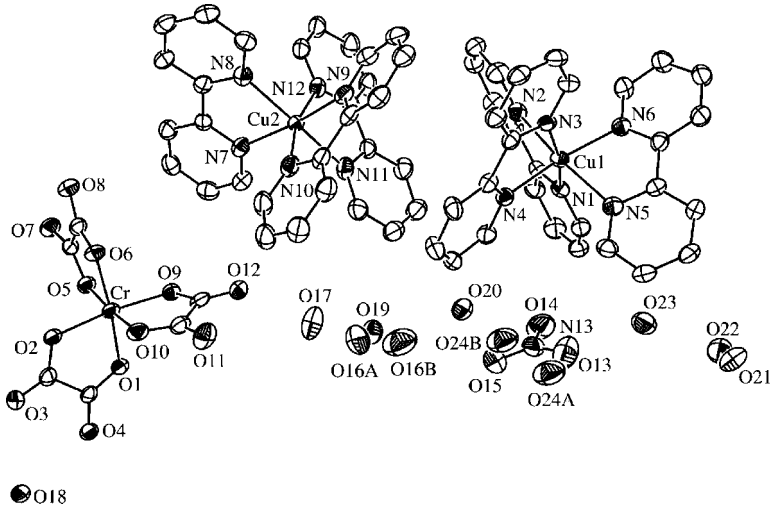

Figure 4. Asymmetric unit of **2** with atom numbering scheme and displacement ellipsoids drawn at the 50% probability level. Two water molecules are disordered over two positions, namely O16A and O16B, O24A and O24B. Occupancies of the oxygen atoms at the A and B sites are 0.84 and 0.16, respectively. Hydrogen atoms are omitted for clarity.

$[Cr(C_2O_4)_3]^{3-}$ anion is very similar to that found in $K_3[Cr(C_2O_4)_3]\cdot 3H_2O$.[22]

Table 3. Selected bond lengths [Å] and angles [°] for compound **2**.

Cu1–N1	2.041(3)	Cu2–N7	2.088(5)
Cu1–N2	2.247(3)	Cu2–N8	2.171(3)
Cu1–N3	2.027(3)	Cu2–N9	2.068(5)
Cu1–N4	2.051(4)	Cu2–N10	2.085(3)
Cu1–N5	2.291(3)	Cu2–N11	2.200(4)
Cu1–N6	2.055(5)	Cu2–N12	2.075(3)
Cr–O1	1.967(3)	Cr–O6	1.964(3)
Cr–O2	1.970(4)	Cr–O9	1.966(4)
Cr–O5	1.982(3)	Cr–O10	1.964(3)
N1–Cu1–N2	77.23(12)	N7–Cu2–N8	77.48(15)
N1–Cu1–N3	169.39(14)	N7–Cu2–N9	169.83(11)
N1–Cu1–N4	95.70(16)	N7–Cu2–N10	97.05(17)
N1–Cu1–N5	97.94(12)	N7–Cu2–N11	96.53(15)
N1–Cu1–N6	92.99(15)	N7–Cu2–N12	91.84(15)
N2–Cu1–N3	93.39(12)	N8–Cu2–N9	93.55(15)
N2–Cu1–N4	95.92(14)	N8–Cu2–N10	95.92(12)
N2–Cu1–N5	171.23(13)	N8–Cu2–N11	171.29(14)
N2–Cu1–N6	96.80(15)	N8–Cu2–N12	96.34(12)
N3–Cu1–N4	80.17(16)	N9–Cu2–N10	78.94(17)
N3–Cu1–N5	91.99(12)	N9–Cu2–N11	92.90(15)
N3–Cu1–N6	93.06(15)	N9–Cu2–N12	93.93(16)
N4–Cu1–N5	91.81(14)	N10–Cu2–N11	91.05(13)
N4–Cu1–N6	165.92(12)	N10–Cu2–N12	166.17(14)
N5–Cu1–N6	75.99(15)	N11–Cu2–N12	77.38(14)
O1–Cr–O2	83.19(14)	O2–Cr–O10	91.86(14)
O1–Cr–O5	92.08(13)	O5–Cr–O6	82.27(12)
O1–Cr–O6	172.95(15)	O5–Cr–O9	95.00(13)
O1–Cr–O9	92.01(14)	O5–Cr–O10	174.71(17)
O1–Cr–O10	92.71(13)	O6–Cr–O9	92.68(15)
O2–Cr–O5	90.94(14)	O6–Cr–O10	93.12(13)
O2–Cr–O6	92.66(14)	O9–Cr–O10	82.59(14)
O2–Cr–O9	172.50(11)		

The crystal structure of **2** consists of hydrophobic and hydrophilic regions. The $[Cu(bpy)_3]^{2+}$ cations are arranged in honeycomb-like hydrophobic layers parallel to $(10\bar{1})$ (Figure 5). The cations are interconnected by the aromatic–aromatic interactions with C···C contact distances in the 3.417(9)–3.598(7) Å range. Each hydrophobic layer is sandwiched between two hydrophilic layers composed of $[Cr(C_2O_4)_3]^{3-}$, nitrate anions and water molecules; all of them are involved in an extensive hydrogen-bonding network (Table 4). The water molecule situated in each hexagonal cell of the "hydrophobic honeycomb" (O18) links two hydrophilic layers by forming hydrogen bonds with the oxalate ligands of $[Cr(C_2O_4)_3]^{3-}$ units from different layers (Figure 6). The crystal structure is additionally stabilised by

Table 4. O–H···O hydrogen-bonding interactions in compound **2**.

D–H···A	D–H [Å]	H···A [Å]	D···A [Å]	D–H···A [°]
O16A–H161···O17	0.84	2.12	2.824(7)	141
O16B–H[a]···O2^{vi}[b]	–	–	2.73(3)	–
O16B–H[a]···O24B	–	–	2.98(5)	–
O17–H171···O19	0.82	2.12	2.910(5)	160
O17–H172···O11	0.86	2.51	3.253(6)	144
O17–H172···O12	0.86	2.24	2.963(5)	141
O18–H181···O3	0.94	2.24	2.874(5)	125
O18–H181···O4	0.94	2.03	2.903(5)	153
O18–H182···O8^{i}	0.72	2.05	2.755(4)	165
O19–H191···O20	0.86	2.10	2.953(6)	172
O19–H192···O9^{ii}	0.84	2.07	2.893(4)	171
O20–H201···O14	0.76	2.19	2.948(6)	172
O20–H202···O5^{ii}	0.88	2.04	2.868(4)	155
O21–H211···O22	0.85	2.12	2.772(4)	133
O21–H212···O2^{iii}	0.85	2.11	2.941(4)	165
O22–H221···O23	0.90	1.90	2.787(5)	170
O22–H222···O7^{iii}	0.90	2.05	2.910(6)	160
O23–H231···O14	0.86	2.26	3.044(7)	151
O23–H[a]···O23^{v}	–	–	2.793(5)	–
O24A–H241···O13	0.86	2.15	2.914(6)	147
O24A–H242···O21^{iv}	0.86	2.17	2.876(6)	139
O24B–H[a]···O13	–	–	2.73(2)	–
O24B–H[a]···O15	–	–	2.71(2)	–
O24B–H[a]···O21^{iv}	–	–	2.77(2)	–

[a] The water hydrogen atom was not found and could not be modelled. [b] Symmetry codes: (i) x, $1/2 - y$, $-1/2 + z$; (ii) $1 - x$, $-y$, $1 - z$; (iii) $-1 + x$, y, $-1 + z$; (iv) $-x$, $1 - y$, $-z$; (v) $-x$, $-y$, $-z$; (vi) $1 - x$, $1 - y$, $1 - z$.

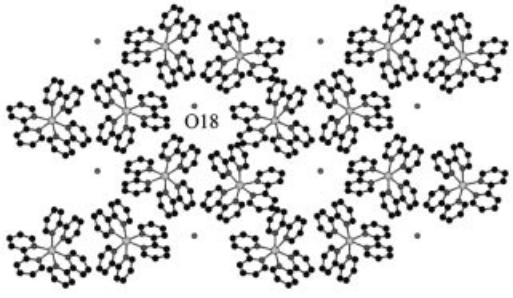

Figure 5. Honeycomb-like layer of $[Cu(bpy)_3]^{2+}$ cations in **2** parallel to $(10\bar{1})$. There is one water molecule (O18) in every hexagonal "honeycomb cell". Hydrogen atoms are omitted for clarity. This view is perpendicular to the layer.

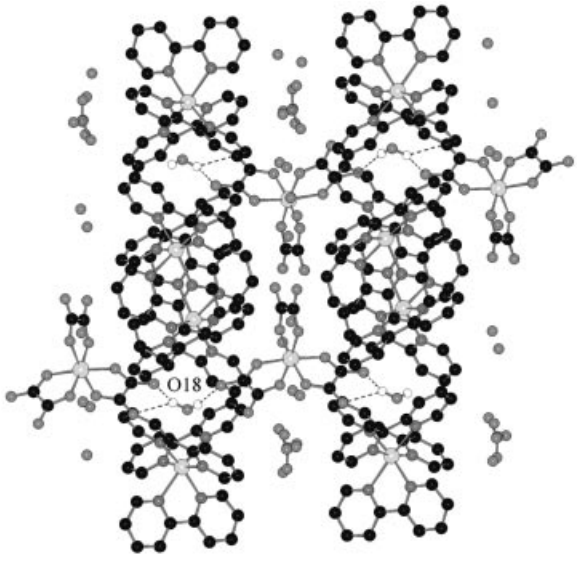

Figure 6. Hydrophobic and hydrophilic layers in **2**. Water molecules bearing the oxygen atoms labelled as O18 link two hydrophilic layers by forming hydrogen bonds (shown by dashed lines) with the oxalate groups of the $[Cr(C_2O_4)_3]^{3-}$ anions. Hydrogen atoms (except those bound to O18) are omitted for clarity. This view is along the *b*-axis.

many C–H···O interactions at the interface between two layers.

The shortest Cu···Cu, Cu···Cr and Cr···Cr distances in the structure of **2** are 7.7558(10) Å [Cu2···Cu2(1 – *x*, –1/2 + *y*, 3/2 – *z*)], 8.0770(10) Å [Cu2···Cr(*x*, 1/2 – *y*, 1/2 + *z*)] and 10.7121(15) Å [Cr···Cr(1 – *x*, –*y*, 1 – *z*)], respectively.

Spectroscopic Properties

Infrared Spectra

Inspection of the IR spectra of **1** and **2** clearly indicates the presence of the absorption bands of the bidentate oxalate group, the bipyridine ligands, the ionic nitrate group and the water molecules in both complexes, in addition to the absorption bands of bis(bidentate) bridging oxalate group in compound **1**. In the spectrum of **1** the absorption bands at: 1717, 1705, 1672, 1663 cm^{-1} [ν_{as}(CO)], 1370, 1251 cm^{-1} [ν_s(CO)] and 801, 795 cm^{-1} [δ(OCO)] are characteristic of bidentate oxalate,[23] whereas those due to the bis(bidentate) bridging oxalate at 1625 cm^{-1} [ν_{as}(CO)], 1338 cm^{-1} [ν_s(CO)] and 817 cm^{-1} [δ(OCO)] agree well with the values reported for dinuclear[8] or tetranuclear[15b] bis(bidentate) bridging oxalate $Cu^{II}Cr^{III}$ complexes. The latter three bands are absent from the spectrum of **2**, and those originating from the bidentate oxalate ligand are found at similar positions as those observed in **1** (see Exp. Sect.).

Electronic Spectra

Electronic spectroscopic data for **1** and **2** were obtained from aqueous solutions and are presented in Table 5. Data for $[Cu(bpy)_3](NO_3)_2{\cdot}6H_2O$ and $K_3[Cr(C_2O_4)_3]{\cdot}3H_2O$ are included for comparison. For the new complexes, the spectra were also recorded as KBr pellets, but this method resulted in essentially the same UV/Vis absorption maxima as those recorded in solution, which indicates that the structures of the complex ions in **1** and **2** are preserved in aqueous media.

The electronic spectra of **1** and **2** exhibit very similar patterns, which confirms the similarity of the local coordination environments around the metal centres in the two complexes. The spectra show the superposition of bands characteristic for both the Cu^{II} and Cr^{III} six-coordinate ions. In the visible region, they are dominated by a broad absorption band with a pronounced shoulder on the lower energy side (of the spectra), which corresponds to the presence of a Cu^{II} ion in a more or less distorted octahedral environment. The unsymmetrical absorption bands for **1** and **2**, having maxima at ca. 715 and ca. 675 nm, respectively, are in good agreement with the spectrum of the starting $[Cu(bpy)_3](NO_3)_2{\cdot}6H_2O$ compound (Table 5), which must have essentially a distorted octahedral geometry. The type of the distortion of the $[Cu(bpy)_3]^{2+}$ ion is significantly dependent on the counteranion present,[18–20] and, in general, does not influence a lot the position of the band maxima. Therefore, the shift of the main absorption maximum in the spectrum of **1** towards the lower energy side relative to the spectrum of **2** could be perceived as a consequence of the different chromophores present in **1** and **2**, namely $[Cu^{I}{}^{I}N_4O_2]$ and $[Cu^{II}N_6]$ (nitrogen ligands exerting higher field strength), rather than as a result of somewhat different geometrical parameters found for Cu^{II} in the two complexes (see Description of the Structures). The presence of an octahedrally coordinated Cr^{III} ion is indicated by the two shoulders, one appearing at the higher energy side of the main visible absorption band (at ca. 565 and 580 nm for **1** and **2**, respectively) and the other observed at the lower energy side of the strong UV band of the spectra (at ca. 415 nm in both cases). The two shoulders in the spectra of **1** and **2** agree well in positions and intensities with the two main absorption bands in the electronic spectrum of $K_3[Cr(C_2O_4)_3]{\cdot}3H_2O$ (maxima appearing at 420 and 570 nm) and can account for the two spin-allowed d–d transitions, $^4A_{2g}(F) \rightarrow {}^4T_{1g}(F)$ and $^4A_{2g}(F) \rightarrow {}^4T_{2g}(F)$, in the octahedral ligand field of a d^3 configuration. An extremely narrow and very weak band observed at ca. 700 nm in both spectra could be ascribed to the spin-forbidden $^4A_{2g} \rightarrow {}^2T_{2g}(F) + {}^2E_g$ transition, characteristic of chromium(III) six-coordinate compounds.

Very strong absorptions (with ε of the order of magnitude of several tens of thousands) in the UV region of the spectra (at ca. 240 and ca. 300 nm) originate from ligand-specific and charge-transfer metal-to-ligand transitions.[24,25]

TG Analysis

As is evidenced from the thermogravimetric analysis, the thermal behaviour of the two compounds is significantly different. Complex **1**, with bridging oxalate groups, is thermally more stable than complex **2**, in both synthetic air and under nitrogen. In synthetic air, the decomposition of **1** starts only after 170 °C by a distinctive step visible in the TG curve and corresponding to the loss of approximately one water molecule (calcd. 1.57%; found 1.75%). The next large step (ca. 58%) in the decomposition curve, in the tem-

Table 5. Electronic spectroscopic data for complexes **1** and **2** and the mononuclear copper(II) and chromium(III) precursor complexes.[a]

Complex	λ_{max} [nm] (ε [$dm^3\,mol^{-1}\,cm^{-1}$])				
	Ligand-specific and CT bands	$^4A_{2g}(F) \rightarrow {}^4T_{1g}(F)$	$^4A_{2g}(F) \rightarrow {}^4T_{2g}(F)$	$^4A_{2g} \rightarrow {}^2T_{2g}(F) + {}^2E_g$	$^2E \rightarrow {}^2A_1$
1	243 (50840), 300 (48800)	413 (sh)	565 (sh)	698 (sh)	715 (120)
2	243 (57640), 297 (54100)	415 (sh)	580 (sh)	697 (sh)	675 (135)
$[Cu(bpy)_3](NO_3)_2{\cdot}6H_2O$	232 (55000), 297 (52000)				680 (130)
$K_3[Cr(C_2O_4)_3]{\cdot}3H_2O$	269 (1500)	420 (105)	568 (87)	697 (8)	

[a] In aqueous solutions.

perature range of ca. 200–300 °C, comprises the removal of bipyridine molecules together with the NO_3^- group. Decomposition of the oxalate groups proceeds in a rather narrow temperature range of 300–400 °C as a strongly exothermic process. Afterwards, the remaining mass stays constant and corresponds to a mixture of copper(II) and chromium(III) oxides.

The elimination of water molecules in **2** proceeds in two well-separated steps taking place in the temperature intervals 40–105 °C and 110–145 °C, both followed by an endothermic peak in the DTA curve. In the first step, six lattice water molecules are expelled (calcd. 6.75%; found 7.05%), the remaining three (calcd. 3.37%; found 3.62%) are lost at higher temperature. The further course of the decomposition process follows that of complex **1**.

Magnetic Properties

The results of magnetic measurements on **1** and **2** are shown in Figure 7, in terms of the dependence of the product of molar susceptibility and temperature, $\chi_M T$, on temperature. The value of $\chi_M T$ for **1** at temperatures above 50 K is almost constant at an average of 2.84 $cm^3 mol^{-1} K$. This corresponds to the effective magnetic moment per molecule $\mu = 4.77\beta$, where β stands for the Bohr magneton. Generally, the spin-only value of the effective magnetic moment for three uncoupled spins is obtained according to the expression:

$$\mu = \beta\sqrt{g_1^2 S_1(S_1 + 1) + g_2^2 S_2(S_2 + 1) + g_3^2 S_3(S_3 + 1)}$$

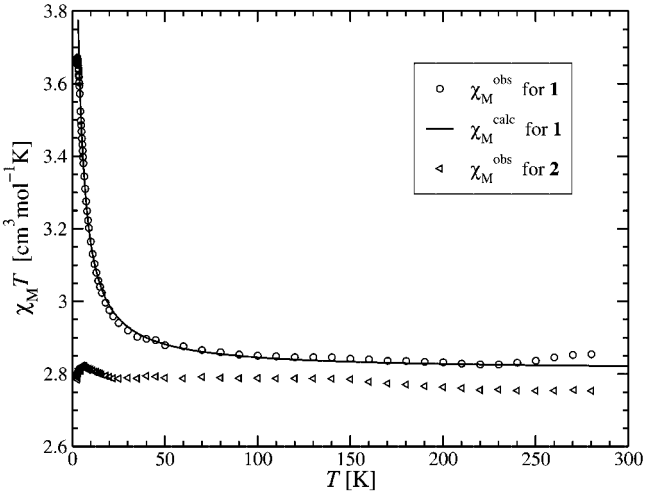

Figure 7. Plots of $\chi_M T$ vs. T for compounds **1** and **2**. The solid line represents the curve of best fit.

For compound **1**, with (S_{Cu1}, S_{Cr}, S_{Cu2}) = (1/2, 3/2, 1/2) and taking $g_{Cu} = g_{Cr} = 2$, the above expression gives a value of $\mu = 4.58\beta$. The measured value is slightly higher and corresponds to $g_{Cu,Cr} = 2.08$. As shown in Figure 7, on cooling the compound below 50 K, the $\chi_M T$ product increases rapidly, and at 2.8 K it attains a value of 3.67 $cm^3 mol^{-1} K$, corresponding to $\mu = 5.42\beta$. This increase of $\chi_M T$ points to the emergence of a ferromagnetic interaction. Below 2.8 K, a very slight decrease of $\chi_M T$ is observed.

The value of the $\chi_M T$ product for **2** at temperatures above 30 K is almost constant and equals 2.77 $cm^3 mol^{-1} K$, which is very close to that of **1**. On cooling the sample below 30 K, first an increase in $\chi_M T$ was observed, but this increase was much smaller than the corresponding increase for **1**. A value of 2.82 $cm^3 mol^{-1} K$ was reached at 5.7 K. With further cooling, the $\chi_M T$ product decreased abruptly to 2.79 $cm^3 mol^{-1} K$ at 3 K. The room temperature effective magnetic moment per molecule for **2** is $\mu = 4.71\beta$. The corresponding g factor which gives this value of μ for the (1/2, 3/2, 1/2) uncoupled spin system is $g_{Cu,Cr} = 2.06$.

The good linear dependences of the reciprocal magnetic susceptibilities, χ_M^{-1}, on temperature (above 50 K) give the Weiss constants ($\theta = 0.8 \pm 0.1$ K for **1** and $\theta = 0.3 \pm 0.1$ K for **2**) which point to a negligible long-range ordering interaction. The absence of a 3D interaction is also in agreement with the value of the effective molecular magnetic moments at the measured temperatures. Therefore, the observed ferromagnetic interaction should be analyzed on the molecular level.

On the basis of the structure of the compound **1** and the magnetic properties of Cu^{II} and Cr^{III} ions, it is reasonable to write the interaction Hamiltonian as in Equation (1):

$$\mathbf{H}_{INT} = -J(S_{Cu1}S_{Cr} + S_{Cu2}S_{Cr}) \quad (1)$$

where J is the exchange interaction between Cu^{II} and Cr^{III} ions in the same molecule, whereas S is the spin operator for the ions labelled by indices.

In the above Hamiltonian only the isotropic Heisenberg exchange term appears, as the Cu^{II} ion does not have zero-field splitting, and for the Cr^{III} ion it is negligible in a first approximation,[1] as shown by the observed magnetic and structural properties. Therefore, the anisotropic and antisymmetric exchange terms are omitted.

Taking $g_{Cu} = g_{Cr} = g$, the following formula is obtained [Equation (2)]:

$$\chi_M = \frac{N\beta^2}{4k}\cdot\frac{g^2}{T}\cdot\frac{10 + e^{-\frac{5J}{2T}} + 10e^{-\frac{J}{T}} + 35e^{\frac{3J}{2T}}}{2 + e^{-\frac{5J}{2T}} + 2e^{-\frac{J}{T}} + 3e^{\frac{3J}{2T}}} \quad (2)$$

The nonlinear fitting of the susceptibility vs. temperature dependence for **1** in the temperature range 2.8–300 K gave the following results: $J = +1.20$ cm^{-1}, $g = 2.07$. The discrepancy factor R, defined as $R = \Sigma[(\chi_M T)_{obsd.} - (\chi_M T)_{calcd.}]^2 / \Sigma[(\chi_M T)_{obsd.}]^2$, equals $1.8 \cdot 10^{-5}$. A small decrease of the magnetic moment below ca. 2.5 K may be generally attributed to an intermolecular antiferromagnetic interaction and/or a zero-field splitting on Cr^{III}.[8,10a]

In order to describe the mechanism of the spin-exchange interaction in oxalate-bridged transition-metal complexes, several models have been considered.[26–28] According to these models only a strict orbital orthogonality results in a ferromagnetic interaction. In the structure of **1** (Figure 1)

the O1 and O1^{i} atoms from the bridging oxalate groups are located in the equatorial planes [consisting of the O1, N2, N3 and N4 atoms for Cu and O1^{i}, N2^{i}, N3^{i} and N4^{i} for Cu^{i} ($i = 1 - x, y, 1/2 - z$)] of the distorted Cu octahedra, whereas the O2 and O2^{i} atoms from the corresponding bridging oxalate ligands occupy the apical positions. The significantly shorter Cu–O1 bond relative to the Cu–O2 bond (Table 1) indicates a strong orbital interaction in the equatorial planes of the two Cu coordination polyhedra, which are mutually related by the twofold axis through the chromium atom. It is clear that the unpaired electron on each copper(II) ion should be described by the $d_{x^2-y^2}$ as the highest energy orbital[1] that will interact with the σ-type oxygen orbitals, forming one of the magnetic orbitals. Simultaneously, the chromium(III) t_{2g} orbitals, with three unpaired electrons, interact with the π-type oxygen orbitals, also resulting in magnetic orbitals. Consequently, a ferromagnetic spin coupling results from the orthogonality of the magnetic orbitals involved. A similar explanation was given for the appearance of a ferromagnetic interaction in [(bpy)(C_2O_4)Cr(μ-C_2O_4)Cu(Hfsaaep)(H_2O)]·2H_2O.[16] In the absence of necessary symmetry conditions, the magnetic interaction in $Cu^{II}Cr^{III}$ oxalate-bridged complexes is antiferromagnetic.[10a,15] For the ferromagnetic $Cu^{II}Cr^{III}Cu^{II}$ compounds mentioned in the introduction,[13a,13b] the values for J were found to be higher than that for **1**. Because the crystal structures of these complexes are still unknown, it is not possible to comment on their J values. Structurally, the coordination environment of Cu^{II} in **1** is similar to that found in the dinuclear compound [(bpy)(C_2O_4)Cr(μ-C_2O_4)-Cu(Hfsaaep)(H_2O)]·2H_2O, for which the ferromagnetic spin-coupling constant $J = +1.4\ cm^{-1}$ (using $\mathbf{H}_{INT} = -JS_{Cu}S_{Cr}$) has been measured.[16] The ferromagnetic interaction with $J = +2.8\ cm^{-1}$ (using $\mathbf{H}_{INT} = -2JS_{Cu}S_{Cr}$) has also been found for the dinuclear complex [Cr(salen)(μ-C_2O_4)Cu(acpy)].[8] The exchange constant ($J = +1.2\ cm^{-1}$) obtained for **1** is comparable to these two values.

Appearance of a slight increase followed by a slight decrease of $\chi_M T$ for the compound **2** when lowering the temperature may come from the zero-field splitting on Cr^{III} and/or from a 3D interaction effect. However, it is not quantitatively well understood at present and is the subject of further investigations.

Conclusion

We have prepared two new heterometallic (Cu^{II} and Cr^{III}) complexes. In **1**, metal atoms are oxalate-bridged in the trinuclear [{Cu(μ-C_2O_4)(bpy)$_2$}$_2$Cr(C_2O_4)]$^+$ cation, whereas **2** consists of two [Cu(bpy)$_3$]$^{2+}$ cations and two {[Cr(C_2O_4)]$^{3-}$ and NO_3^-} anions. Compound **1** is the first trinuclear $Cu^{II}Cr^{III}Cu^{II}$ complex with solved crystal structure. This fact allowed us to explain the pathway of a ferromagnetic exchange interaction between the Cu^{II} and Cr^{III} metal ions mediated through the bridging oxalate groups. We are currently engaged in a more detailed study aiming to understand the magnetic behaviour of **2** at low temperature.

Experimental Section

General Remarks: All the reagents used in the syntheses were purchased from commercial sources and used without further purification. K$_3$[Cr(C_2O_4)$_3$]·3H_2O and [Cu(bpy)$_3$](NO_3)$_2$·6H_2O were prepared according to the literature methods.[29,30]

Synthesis of [{Cu(μ-C_2O_4)(bpy)$_2$}$_2$Cr(C_2O_4)]NO_3·H_2O (1): To an aqueous solution (15 mL) of K$_3$[Cr(C_2O_4)$_3$]·3H_2O (146.7 mg, 0.301 mmol) were added an aqueous solution (12 mL) of Cu(NO_3)$_2$·3H_2O (145.8 mg, 0.603 mmol) and an ethanolic solution (10 mL) of bpy (188.4 mg, 1.206 mmol) dropwise with stirring at room temperature. Slow concentration of the resulting solution at ambient conditions led to the formation of dark-green single crystals of **1** as the only solid with a yield of 297.1 mg (86%). $C_{46}H_{34}CrCu_2N_9O_{16}$ (1147.90): calcd. C 48.13, H 2.98, N 10.98; found C 47.74, H 3.14, N 10.93. IR data (KBr): $\tilde{\nu}$ = 3434 (w, br), 3073 (w), 1717 (m), 1705 (m), 1672 (vs), 1663 (vs), 1625 (vs), 1607 (m), 1598 (s), 1493 (m), 1474 (m), 1444 (s), 1415 (s), 1382 (vs), 1370 (sh), 1338 (m), 1314 (m), 1276 (m), 1251 (m), 1226 (m), 1175 (w), 1162 (w), 1105 (w), 1029 (w), 1013 (w), 898 (w), 817 (sh), 801 (m), 795 (m), 773 (vs), 732 (m), 534 (m), 460 (w), 419 (m), 410 (m), 304 (w) cm^{-1}.

Synthesis of [Cu(bpy)$_3$]$_2$[Cr(C_2O_4)$_3$]NO_3·9H_2O (2): To an aqueous solution (15 mL) of K$_3$[Cr(C_2O_4)$_3$]·3H_2O (103.3 mg, 0.212 mmol) was added an aqueous solution (10 mL) of [Cu(bpy)$_3$](NO_3)$_2$·6H_2O (162.0 mg, 0.212 mmol) dropwise with stirring at room temperature. The green-blue plate-like crystals of **2** were formed in the solution in a period of three days. The yield was 125.8 mg (37%, based on Cr). $C_{66}H_{66}CrCu_2N_{13}O_{24}$ (1604.40): calcd. C 49.41, H 4.15, N 11.35; found C 49.14, H 4.40, N 11.71. IR data (KBr): $\tilde{\nu}$ = 3415 (m, br), 3074 (w), 1708 (m), 1681 (s), 1650 (m), 1594 (m), 1491 (w), 1472 (m), 1441 (s), 1384 (vs), 1372 (m), 1312 (w), 1257 (sh), 1248 (m), 1176 (w), 1158 (w), 1101 (w), 1062 (w), 1043 (w), 1015 (m), 910 (w), 806 (m), 797 (m), 776 (vs), 734 (m), 650 (m), 538 (m), 475 (w), 411 (m), 307 (w) cm^{-1}.

When the reaction of K$_3$[Cr(C_2O_4)$_3$]·3H_2O and [Cu(bpy)$_3$](NO_3)$_2$·6H_2O was performed in a molar ratio of 1:2, crystals of both **1** and **2** formed simultaneously.

Physical Techniques: Infrared absorption spectra were recorded by using KBr pellets with an ABB Bomem FT model MB 102 spectrometer, in the 4000–200 cm^{-1} region. Thermogravimetric measurements were carried out with a Shimadzu DTG-60 analyzer, with a heating rate of 10 °C min^{-1} in a stream of synthetic air. Electronic spectra were measured with a Cary 50 Probe spectrophotometer. Solution spectra were recorded in H_2O by using 1-cm silica cells. For solid-state spectra, the samples were prepared as KBr pellets which were mounted in the pathway of the radiation beam. A weighed pure-KBr pellet was used as the reference.

Magnetic moments were measured with a commercial SQUID magnetometer (MPMS-5, Quantum Design). Measurements were performed in the temperature range 1.8–290 K at an applied magnetic field of 1 T. The field dependence of the magnetic moment was checked up to 5 T, and both samples showed linearity up to more than 1 T even at 2 K, so the susceptibilities analyzed here are field-independent. The calculated molar magnetic susceptibilities were corrected for the diamagnetic contributions of the constituent atoms, which are $-560 \cdot 10^{-6}\ cm^3\ mol^{-1}$ for **1** and $-874 \cdot 10^{-6}\ cm^3\ mol^{-1}$ for **2** according to Pascal's constants.[31] Also, a correction was made for temperature-independent paramagnetism, which is $110 \cdot 10^{-6}\ cm^3\ mol^{-1}$ for Cr^{III} and $60 \cdot 10^{-6}\ cm^3\ mol^{-1}$ for Cu^{II} ions.[10d]

X-ray Crystallographic Study: Each of the selected single crystals of **1** and **2** was glued on the tip of a glass fibre and coated with a

thin layer of silicone grease. The X-ray data were collected at 100(1) K by ω scans with an Oxford Diffraction Xcalibur 3 CCD diffractometer with graphite-monochromated Mo-K_α radiation (λ = 0.71073 Å). Data reduction including the absorption correction was performed with the CrysAlis software package.[32] Crystal data, experimental conditions and final refinement parameters are summarized in Table 6. Solution, refinement and analysis of the structures was performed by using the programs integrated in the WinGX system.[33] Both structures were solved by direct methods (SIR92)[34] and refined by the full-matrix least-squares method based on F^2 against all reflections (SHELXL-97).[35] All non-hydrogen atoms were refined anisotropically. The anisotropic displacement parameters of the disordered atoms were restrained during refinement, except those of the atoms C23B in **1** and O24B in **2** which were constrained to equal the anisotropic displacement parameters of C23A and O24A, respectively (EADP). Additionally, in **1**, the geometries of the two parts of the disordered non-bridging oxalate ligands were restrained to be equal. Furthermore, the atoms in each of the sets {O5, O6A, C23A, C23B($1-x$, y, $1/2-z$)} and {O5, O6B, C23B, C23A($1-x$, y, $1/2-z$)} were restrained to be coplanar. In both structures, the hydrogen atoms bound to the carbon atoms were treated as riding in idealized positions, with C–H = 0.95 Å, and displacement parameters were assigned as $U_{iso}(H) = 1.2U_{eq}$ of the attached C atom. Initial positions of the water H atoms in **1** as well as those of some of the H atoms of the water molecules in **2** were found in the difference Fourier map. Other modelled water H atoms of **2** were obtained by combined geometric and force-field calculations on the basis of hydrogen-bonding interactions (CALC-OH).[36] For all water H atoms, the O–H vector directions were kept fixed, while the O–H distances were restrained (DFIX 0.85 0.02) during refinement. Prior to applying the mentioned constraints and restraints to the water molecules, those having the calculated H atoms were additionally refined as rigid bodies by using the O atoms as the pivot ones. Displacement parameters of all water H atoms were assigned as $U_{iso}(H) = 1.5U_{eq}$ of the joined O atom. Geometrical calculations were performed using PLATON[37] and the figures were produced by using ORTEP-3[38] and SCHAKAL99.[39]

Table 6. Crystallographic data for compounds **1** and **2**.

Compound	**1**	**2**
Empirical formula	$C_{46}H_{34}CrCu_2N_9O_{16}$	$C_{66}H_{66}CrCu_2N_{13}O_{24}$
M_r	1147.90	1604.40
Crystal colour, habit	dark green prism	green-blue prism
Crystal size [mm]	0.48×0.21×0.20	0.44×0.24×0.15
Crystal system	monoclinic	monoclinic
Space group	*C*2/*c* (no. 15)	$P2_1/c$ (no. 14)
a [Å]	16.4284(12)	31.314(3)
b [Å]	17.1622(11)	13.5356(11)
c [Å]	16.7494(12)	22.202(2)
β [°]	110.721(7)	132.012(13)
V [Å^3]	4417.0(6)	6992.0(18)
Z	4	4
T [K]	100(1)	100(1)
$D_{calcd.}$ [g cm^{-3}]	1.726	1.524
μ (Mo-K_α) [mm^{-1}]	1.285	0.845
Absorption correction	numerical	numerical
T_{min}/T_{max}	0.659/0.816	0.710/0.896
F(000)	2332	3308
θ range for collected data [°]	4.15–30.00	3.88–25.00
Limiting indices	$-23 \le h \le 23$	$-37 \le h \le 37$
	$-24 \le k \le 24$	$-16 \le k \le 15$
	$-23 \le l \le 23$	$-26 \le l \le 26$
Data total/unique	34029/6427	85275/12253
R_{int}/R_σ	0.0238/0.0245	0.0500/0.0356
Completeness to θ_{max}	0.997	0.995
Observed data [$I > 2\sigma(I)$]	5450	10113
Data/restraints/parameters	6427/37/370	12253/16/977
S/restrained *S*	1.113/1.111	1.156/1.160
R_1, wR_2 [$I > 2\sigma(I)$]	0.0357, 0.0896	0.0570, 0.1496
R_1, wR_2 (all data)	0.0456, 0.0930	0.0753, 0.1637
$\Delta\rho_{max}$ [e Å^{-3}]	0.748	1.116
$\Delta\rho_{min}$ [e Å^{-3}]	–0.413	–0.647

CCDC-279737 (**1**) and CCDC-279738 (**2**) contain the supplementary crystallographic data for this paper. These data can be obtained free of charge from The Cambridge Crystallographic Data Centre via www.ccdc.cam.ac.uk/data_request/cif.

Supporting Information (see footnote on the first page of this article): All hydrogen-bonding interactions in the structure of **1** (Table S1) and the structure of **2** (Table S2).

Acknowledgments

This research was supported by the Ministry of Science, Education and Sports of the Republic of Croatia (Grants No. 0098066, 0119632 and 0119258).

[1] O. Kahn, *Molecular Magnetism*, Wiley-VCH, New York, **1993**.
[2] W. Linert, M. Verdaguer (Eds.), *Molecular Magnets Recent Highlights*, Springer-Verlag, Wien, **2003**.
[3] a) H. Tamaki, Z. J. Zhong, N. Matsumoto, S. Kida, M. Koikawa, N. Achiwa, Y. Hashimoto, H. Ōkawa, *J. Am. Chem. Soc.* **1992**, *114*, 6974–6979; b) Z. J. Zhong, N. Matsumoto, H. Ōkawa, S. Kida, *Chem. Lett.* **1990**, 87–90.
[4] a) L. O. Atovmyan, G. V. Shilov, R. N. Lyubovskaya, E. I. Zhilyaeva, N. S. Ovanesyan, S. I. Pirumova, I. G. Gusakovskaya, Y. G. Morozov, *JETP Lett.* **1993**, *58*, 766–769; b) R. Pellaux, H. W. Schmalle, R. Huber, P. Fischer, T. Hauss, B. Ouladdiaf, S. Decurtins, *Inorg. Chem.* **1997**, *36*, 2301–2308.
[5] S. Decurtins, H. W. Schmalle, H. R. Oswald, A. Linden, J. Ensling, P. Gütlich, A. Hauser, *Inorg. Chim. Acta* **1994**, *216*, 65–73.
[6] a) S. Decurtins, H. W. Schmalle, P. Schneuwly, J. Ensling, P. Gütlich, *J. Am. Chem. Soc.* **1994**, *116*, 9521–9528; b) S. Decurtins, H. W. Schmalle, R. Pellaux, P. Schneuwly, A. Hauser, *Inorg. Chem.* **1996**, *35*, 1451–1460; c) R. Sieber, S. Decurtins, H. Stoeckli-Evans, C. Wilson, D. Yufit, J. A. K. Howard, S. C. Capelli, A. Hauser, *Chem. Eur. J.* **2000**, *6*, 361–368.
[7] a) E. Coronado, J. R. Galán-Mascarós, C. J. Gómez-García, J. M. Martínez-Agudo, *Inorg. Chem.* **2001**, *40*, 113–120; b) R. Andrés, M. Brissard, M. Gruselle, C. Train, J. Vaissermann, B. Malézieux, J.-P. Jamet, M. Verdaguer, *Inorg. Chem.* **2001**, *40*, 4633–4640.
[8] M. Ohba, H. Tamaki, N. Matsumoto, H. Ōkawa, *Inorg. Chem.* **1993**, *32*, 5385–5390.
[9] T. Sanada, T. Suzuki, T. Yoshida, S. Kaizaki, *Inorg. Chem.* **1998**, *37*, 4712–4717.
[10] a) M. Andruh, R. Melanson, C. V. Stager, F. D. Rochon, *Inorg. Chim. Acta* **1996**, *251*, 309–317; b) F. D. Rochon, R. Melanson, M. Andruh, *Inorg. Chem.* **1996**, *35*, 6086–6092; c) M. C. Muñoz, M. Julve, F. Lloret, J. Faus, M. Andruh, *J. Chem. Soc., Dalton Trans.* **1998**, 3125–3131; d) R. Lescouëzec, G. Marinescu, J. Vaissermann, F. Lloret, J. Faus, M. Andruh, M. Julve, *Inorg. Chim. Acta* **2003**, *350*, 131–142.
[11] G. Marinescu, M. Andruh, R. Lescouëzec, M. C. Muñoz, J. Cano, F. Lloret, M. Julve, *New J. Chem.* **2000**, *24*, 527–536.
[12] G. De Munno, D. Armentano, M. Julve, F. Lloret, R. Lescouëzec, J. Faus, *Inorg. Chem.* **1999**, *38*, 2234–2237.
[13] a) Y.-T. Li, C.-W. Yan, H.-S. Guan, *Polyhedron* **2003**, *22*, 3223–3230; b) Y.-T. Li, C.-W. Yan, J.-F. Lou, H.-S. Guan, *J. Magn. Magn. Mater.* **2004**, *281*, 68–76; c) Y.-T. Li, C.-W. Yan, H.-S. Guan, *Transition Met. Chem.* **2004**, *29*, 537–542.

[14] F. H. Allen, O. Kennard, D. G. Watson, L. Brammer, A. G. Orpen, R. Taylor, *J. Chem. Soc., Perkin Trans. 2* **1987**, S1–S19.
[15] a) O. Costisor, K. Mereiter, M. Julve, F. Lloret, Y. Journaux, W. Linert, M. Andruh, *Inorg. Chim. Acta* **2001**, *324*, 352–358; b) E. Coronado, M. C. Giménez, C. J. Gómez-García, F. M. Romero, *Polyhedron* **2003**, *22*, 3115–3122.
[16] G. Marinescu, D. Visinescu, A. Cucos, M. Andruh, Y. Journaux, V. Kravtsov, Y. A. Simonov, J. Lipkowski, *Eur. J. Inorg. Chem.* **2004**, 2914–2922.
[17] C. Janiak, *J. Chem. Soc., Dalton Trans.* **2000**, 3885–3896.
[18] C. Faulmann, Y. S. J. Veldhuizen, J. G. Haasnoot, J. Reedijk, P. Cassoux, *Acta Crystallogr., Sect. C* **1998**, *54*, 1827–1830.
[19] P. Majumdar, A. K. Ghosh, L. R. Falvello, S.-M. Peng, S. Goswami, *Inorg. Chem.* **1998**, *37*, 1651–1654.
[20] J.-L. Song, H.-Y. Zeng, B.-P. Yang, Z.-C. Dong, G.-C. Guo, J.-S. Huang, *Jiegou Huaxue* **2003**, *22*, 29.
[21] G. A. van Albada, A. Mohamadou, I. Mutikainen, U. Turpeinen, J. Reedijk, *Eur. J. Inorg. Chem.* **2004**, 3733–3742.
[22] D. Taylor, *Aust. J. Chem.* **1978**, *31*, 1455.
[23] K. Nakamoto, *Infrared and Raman Spectra of Inorganic and Coordination Compounds*, 5th ed., John Wiley, New York, **1997**.
[24] D. Sutton, *Electronic Spectra of Transition Metal Complexes*, McGraw-Hill, London, **1968**.
[25] A. B. P. Lever, *Inorganic Electronic Spectroscopy*, Elsevier, Amsterdam, **1968**.
[26] M. Julve, M. Verdaguer, A. Gleizes, M. Philoche-Levisalles, O. Kahn, *Inorg. Chem.* **1984**, *23*, 3808–3818.
[27] Y. Pei, Y. Journaux, O. Kahn, *Inorg. Chem.* **1989**, *28*, 100–103.
[28] J. Cano, P. Alemany, S. Alvarez, M. Verdaguer, E. Ruiz, *Chem. Eur. J.* **1998**, *4*, 476–484.
[29] G. Brauer (Ed.), *Handbuch der Präparativen Anorganischen Chemie*, Ferdinand Enke Verlag, Stuttgart, **1954**.
[30] F. M. Jaeger, J. A. van Dijk, *Z. Anorg. Allg. Chem.* **1936**, *227*, 273–327.
[31] P. W. Selwood, *Magnetochemistry*, Interscience Publishers, Inc., New York, **1956**.
[32] Oxford Diffraction, Oxford Diffraction Ltd., *Xcalibur CCD System, CrysAlis Software System*, Version 1.170, **2003**.
[33] L. J. Farrugia, *J. Appl. Crystallogr.* **1999**, *32*, 837–838.
[34] A. Altomare, G. Cascarano, C. Giacovazzo, A. Guagliardi, *J. Appl. Crystallogr.* **1993**, *26*, 343–350.
[35] M. Sheldrick, *SHELXL-97, Program for the Refinement of Crystal Structures*, University of Göttingen, Germany, **1997**.
[36] M. Nardelli, *J. Appl. Crystallogr.* **1999**, *32*, 563–571.
[37] a) A. L. Spek, *Acta Crystallogr., Sect. A* **1990**, *46*, C34; b) A. L. Spek, *PLATON – A Multipurpose Crystallographic Tool*, Utrecht University, Utrecht, The Netherlands, **2005**.
[38] L. J. Farrugia, *J. Appl. Crystallogr.* **1997**, *30*, 565.
[39] E. Keller, *J. Appl. Crystallogr.* **1989**, *22*, 19–22.

Received: December 6, 2005
Published Online: April 25, 2006

